Microstructural evolution and characterisation of interfacial phases in Al_2O_3/Ag–Cu–Ti/Al_2O_3 braze joints

M. Ali[a,*], K. M. Knowles[a], P. M. Mallinson[b], J. A. Fernie[b]

[a]Department of Materials Science and Metallurgy, University of Cambridge, 27 Charles Babbage Road, Cambridge, CB3 0FS, UK
[b]Materials Science, AWE, Aldermaston, Reading, Berkshire, RG7 4PR, UK
*Corresponding author: Tel.: +44 (0)1223 334357
E-mail address: ma591@cam.ac.uk

Abstract

Alumina ceramics with different levels of purity have been joined to themselves using an active braze alloy (ABA) Ag–35.3Cu–1.8Ti wt% and brazing cycles that peak at temperatures between 815°C and 875°C for 2 to 300 min. The microstructures of the joints have been studied using scanning electron microscopy (SEM), transmission electron microscopy (TEM), and energy dispersive X-ray spectroscopy (EDS). A limited number of joints prepared with the ABA Ag–26.7Cu–4.5Ti wt% have also been studied. In terms of characterising the interfacial phases, efforts were made to understand the interfacial reactions, and to determine the influence of various brazing parameters, such as the peak temperature (T_p) and time at T_p (τ), on the microstructure. In addition, the extent to which impurities in the alumina affect the interfacial microstructure has been determined.

Ti_3Cu_3O has been identified as the main product of the reactions at the ABA/alumina interfaces. At the shortest joining time used, this phase was observed in the form of a micron-size continuous layer in contact with the ABA, alongside a nanometre-size layer on the alumina that was mostly composed of γ−TiO grains. Occasionally, single grains of Ti_3O_2 were observed in the thin layer on alumina. In the joints prepared with Ag–35.3Cu–1.8Ti wt%, the interfacial structure evolved considerably with joining time, eventually leading to a high degree of inhomogeneity across the length of the joint at the highest T_p. The level of purity of alumina was not found to affect the overall interfacial microstructure, which is attributed to the formation of various solid solutions. It is suggested that Ti_3Cu_3O forms initially on the alumina. Diffusion of Ti occurs subsequently to form titanium oxide at the Ti_3Cu_3O/alumina interface.

1. Introduction

Alumina ceramics are often joined to metals to form assemblies with a diverse range of applications, such as vacuum feedthrough technology for high voltage and pressure environments, semiconductor housing and accelerator, plasma and laser technologies

[1]. Applications for alumina–alumina joints are more limited. These joints are usually made when ceramic components with complex geometries are required [2].

The various methods for fabricating ceramic to ceramic and ceramic to metal joints for several engineering ceramics have been recently reviewed [3]. Of these, brazing is a relatively simple and versatile technique to join similar and dissimilar materials (notwithstanding any issues relating to joint design). Currently, there are two commonly used brazing techniques in industry to join alumina ceramics to metals and to themselves. These are active metal brazing (AMB) and sintered metal powder processing (SMPP); the most commonly known variant of SMPP being the moly–manganese (Mo-Mn) process. The Mo–Mn process was originally developed for zirconium silicate, magnesium silicate and oxide ceramics such as alumina containing a glassy secondary phase [4]. It is a multi-step process, which is achieved by modifying the bonding surfaces of the ceramic to render them more wettable by a conventional braze alloy, such as the Ag–28Cu wt% eutectic alloy. Hey [5] has discussed several practical aspects of this process relating to the preparation of the ceramic, the composition and application of the primary metallising layer, and subsequent firing, plating and further heat treatment steps. The Mo–Mn process is lengthy and considerably more complex than AMB. During AMB, joining is achieved in a single step using an alloy that has been chemically modified with the addition of an element to cause precipitation of intermetallic compounds at the braze alloy/alumina interface. These interfacial phases are wetted by the braze alloy, and so their formation can be considered as an in-situ metallisation process. The element added is commonly known as an active element and the resultant braze alloy is called an active braze alloy (ABA).

The majority of alumina brazing studies have used ABAs based on the Ag–Cu system activated by small amounts of Ti, typically ranging from 1–5 wt%. Other group IV and V elements such as Zr, Hf and V can also be added to Ag, Cu and Ag–Cu alloys [6,7,8,9], but the resultant binary and ternary ABAs have received far less attention than the Ag–Cu–Ti system. By comparison, X-ray diffraction (XRD) and electron microscopy investigations to characterise the reaction products at Ag–Cu–Ti thin foil/Al_2O_3 interfaces have been numerous. A large selection of reports on the interfacial phases that have formed using various joining conditions in the Al_2O_3/Ag–Cu–Ti/Al_2O_3 system are summarised in Table 1; the studies are arranged so that the concentration of Ti in the Ag–Cu–Ti alloy is increasing, and, for the same concentration of Ti, the peak joining temperature is also increasing.

A common characteristic in the majority of these studies is the formation of a micrometre-size reaction bilayer at the interface, which is typically reported as being composed of a Ti_xO_y compound in the form of a thin continuous layer on alumina, along with a thicker M_6O layer, where M is a mixture of Ti and Cu, in contact with the braze alloy. However, there are several points of disagreement on the stoichiometry of Ti_xO_y and M_6O that form. For example, Hahn et al. [10] suggested $TiO_{1.04}$ and Ti_4Cu_2O form by heat treating 96 wt% α–Al_2O_3 with Ag–33.5Cu–1.5Ti wt% at 830°C for 10 minutes, while Stephens et al. [11] found evidence for γ–TiO and Ti_3Cu_3O when a similar ABA (Ag–34.1Cu–1.7Ti wt%) was held at 845°C

for 6 minutes on sapphire. In a more recent study, Lin et al. [12] found evidence for Ti_3O_2 (designated Ti_2O) and Ti_3Cu_3O at a 99.9 wt% α–Al_2O_3/Ag–26.7Cu–4.5Ti wt% interface, which was held at 915°C for 20 min. In addition, various binary compounds such as Cu_2O [13], AlTi and $CuTi_2$ [14] have been reported.

The inconsistencies in the reported data have provided motivation for the current work to establish conclusively, using transmission electron microscopy (TEM) and electron diffraction, the nature of the interfacial reaction products by performing a comprehensive evaluation of a number of joints, prepared using a wide range of conditions. TEM is an excellent experimental technique to observe directly the morphology of the individual grains in the reaction layer(s) and to determine their crystal structure. The main objective of this work has been to acquire a better understanding of the evolution of the interfacial phases. The fundamental physical processes that occur at this ABA/alumina interface, along with the influence of brazing parameters such as the peak temperature (T_p) and time at T_p (τ) on the microstructure of joints, are not fully understood. This is apparent from the conflicting nature of the bonding mechanisms suggested in the literature [11,12,15]. Another aspect of this work has been to determine the extent to which secondary/glassy phases in alumina participate in the interfacial reactions, (the cost of alumina ceramics is strongly dependent on the purity level). There is no clear evidence in the literature that shows if the grain boundary microstructure in alumina is, or is not, important.

A systematic approach to evaluate the microstructure of a range of Al_2O_3/Ag–Cu–Ti/Al_2O_3 joints has been undertaken. Joints have been prepared using three different grades of alumina, two Ag–Cu–Ti ABAs, four peak joining temperatures, ranging from 815°C to 900°C, and joining times ranging from 2 min to 300 min. The selection of conditions used also includes joining times that simulate conditions used in commercial practice. The effects of altering the purity of alumina, T_p and τ on the microstructure of the joints have been studied and a mechanism for the formation of the interfacial phases has been proposed.

2. Experimental

2.1. Materials

Two commercially available Ag–Cu–Ti based ABAs were used to join different grades of alumina to themselves. The majority of the joints were prepared using Cusil ABA (Ag–35.3Cu–1.8Ti wt%). A limited number of joints were prepared with Ticusil (Ag–26.7Cu–4.5Ti wt%). Both ABAs were used in foil form, with a thickness of ~50 μm, from which material was punched to prepare ABA preforms for joining. XRD, scanning electron microscopy (SEM) and energy dispersive X-ray spectroscopy (EDS) investigations of the as-received ABAs revealed different microstructures. A cross-section of Cusil ABA contained grains of Cu_4Ti randomly distributed amongst the Ag–Cu eutectic alloy, as shown in the back scattered electron image (BSEI) given

in Figure 1a. Ticusil was composed of a Ag–Cu eutectic/Ti/Ag–Cu eutectic sandwich structure as shown in Figure 1b. The thickness of the Ti layer was not uniform across the length of the cross-sections examined and varied between ~50 nm and ~5 μm. There was evidence of reaction between Ti and Cu in isolated regions along the Ti/Ag–Cu interfaces, where Cu_4Ti_3 was observed.

Braze joints made with high purity 99.7 wt% α–Al_2O_3, which is designated A99 here, were compared with those made with two different grades of 95.0 wt% α–Al_2O_3. One of the 95.0 wt% α–Al_2O_3 grades contained SiO_2 as the main secondary phase and is designated A95. This alumina also contained ZrO_2 which was randomly distributed throughout it. One explanation for the presence of ZrO_2 is that it was transferred to alumina powder during a milling process that employed ZrO_2 grinding media to produce fine alumina powder prior to sintering. The other 95.0 wt% α–Al_2O_3 contained calcium silicate as the main secondary phase and is designated B95. Electron microprobe analysis was performed on the bonding surfaces of these ceramics to determine their composition, after polishing using standard metallographic techniques and coating with a thin layer of carbon. A Cameca SX-100 (France) electron microprobe operated at 15 keV with a 10 nA electron beam was used in the wavelength-dispersive mode. Calibration of the elements of interest used several mineral standards. The composition of each alumina is given in Table 2.

The initial grain sizes of the alumina ceramics were typically between 3 and 10 μm. SEM work shown in Section 3.1.2 indicated that secondary phases at the grain boundaries in the ceramics did not affect the interfacial microstructure in the joints. A variation in the initial grain size of alumina in this range is therefore not expected to affect interfacial phase formation significantly.

ASTM F19-64 [26] tensile button samples were prepared by joining each grade of alumina to itself, as shown in Figure 2. The apparent surface area of the substrates was ~1.2×10^{-4} m^2, which agreed with the structure of the ABA preforms. A profilometer (Dektak 6M stylus profiler, Veeco, USA) was used to measure the average surface roughness (R_a) of the as received alumina components. R_a values were ~2.1 μm, ~1.3 μm and ~0.6 μm for A99, A95 and B95 respectively. Prior to brazing, the alumina components and ABAs were immersed in detergent and placed in an ultrasonic bath for up to ~15 min.

2.2. Brazing Processes

Brazing procedures were performed in either vacuum or argon. Three furnaces that were capable of maintaining a vacuum of 10^{-5} mbar or better at T_p were regularly used to prepare joints with Cusil ABA. A limited number of joints made with this ABA and those with Ticusil were prepared in argon. A list of the joints prepared with Cusil ABA and the joining environments used are given in Table 3.

For vacuum brazing experiments with T_p between 815°C and 875°C, τ ranged from 2 min to 300 min. In all cases in Table 3, a 30 min dwell period was incorporated into the brazing cycle on heating to 750°C, to help reduce any temperature gradients across the components. The heating rates were ~10°C min^{-1} and the cooling rate was

~10°C min^{-1} between T_p and ~450°C, followed by a furnace cool to room temperature. A pressure of ~225 Pa was applied to the joints via a 50 g weight. Duplicate samples were prepared at T_p of 815°C and τ of 2 min with A95 to monitor the reproducibility of the brazing process, which was found to be good. There were no significant differences between the microstructures of these joints.

For brazing experiments in argon, a horizontal electric furnace was used (STF 15/450, Carbolite, UK). Argon gas was purified using the BIP® technology by Air Products and Chemicals (USA), after which it was then introduced to the furnace. This purification process reduces the concentrations of O_2 and H_2O to less than 10 and 20 ppb respectively. A purging procedure that involved evacuating the furnace to a rough vacuum before cleaning with purified argon was repeated three times to prepare the furnace for brazing experiments. The profile of the brazing cycle used was very similar to that used in the vacuum brazing experiments described above. Here, the heating rate was ~9°C min^{-1}, and the cooling rates were ~9°C min^{-1} between T_p and ~450°C, and significantly lower during a furnace cool to room temperature. Although the joints would have been held at temperatures close to T_p for slightly longer, those made with Cusil ABA could not be differentiated microstructurally from those made with the same ABA, T_p and τ in vacuum. Therefore, it was concluded that the difference in joining environment was not crucial to the development of the reaction products in the Al_2O_3/Cusil ABA/Al_2O_3 joint. While brazing with Ticusil, samples were held at T_p of 900°C for 2, 15 and 30 min. A pressure of ~225 Pa was applied to all of the joints prepared in argon.

To examine the reactivity and thermal stability of the reaction products at the Cusil ABA/Al_2O_3 interface, annealing procedures were performed on 6 mm × 3 mm × 5 mm sections of an B95/Cusil ABA/B95 joint, which was previously prepared in vacuum by holding for 2 min at 815°C. The sections were sealed in clean quartz tubes, which were thoroughly rinsed with detergent (a solution of 10% HNO_3 in distilled water) and distilled water before being fired at 350°C overnight. Before sealing, the tubes were purged using a similar process to that described above, and then filled with argon. Samples were heat treated at 815°C for 5 to 150 h in an electric chamber furnace (UAF 15/5, Lenton, UK). Long heat treatment times were used to understand the development of the interfacial phases and enable the formation of coarser grains at the interface, which could then be analysed by EDS in the SEM.

2.3. Analytical procedures

Several electron microscopy techniques were used in this investigation. Three (or more) cross-sections from each joint were analysed using a field emission SEM (Leo 1530 VP, Leo Electron Microscopy - Carl Zeiss, Germany) operated at 20 keV and equipped with an energy dispersive spectrometer (INCA-7426, Oxford Instruments, UK) to monitor the homogeneity of the interfacial morphology and chemistry across the joint. Samples for SEM analysis were mounted in an acrylic polymer at room temperature, polished using standard metallographic techniques and finally coated with a thin layer of carbon. Monte-Carlo simulations performed on a flat Ti_3Cu_3O

specimen (density, ρ, of 6.52 g cm^{-3}) suggested an accelerating voltage of 20 keV would generate an interaction volume with a depth and width of ~1 μm. As this volume was significantly larger than the typical width of a Ti_xO_y layer found on alumina, elemental analysis was also performed on thin films in a scanning transmission electron microscope, STEM, (Tecnai Osiris, FEI, USA). This microscope was operated at 200 keV and equipped with an EDS system employing four windowless Bruker silicon drift detectors (Super-X system, FEI, USA), which permitted the acquisition of weak and low energy X-rays such as O K_α. Thin films were extracted from the joints using a focussed ion beam instrument (Helios Nanolab, FEI, USA). A standard procedure [27], commonly known as the lift-out technique, was used to transfer ~15 μm × ~10 μm cross-sections of the Ag–Cu–Ti/Al_2O_3 interfaces to Mo grids, or a carbon substrate on a Mo grid, before reducing their thickness to ~100 nm.

A high angle annular dark field (HAADF) detector was used in the STEM for atomic number contrast imaging of the thin films. This contrast mechanism helped to identify small volumes of Ag-rich braze adjacent to, and inside, the Ti_xO_y layer. It was important to have a good knowledge of the distribution of the Ag-rich phase in this layer before collecting electron diffraction data from the Ti_xO_y particles. This is because the Ag-rich phase had the same Bravais lattice and a very similar unit cell length as γ–TiO, which is a commonly observed Ti_xO_y phase. Selected area diffraction techniques were used to determine the crystal structure of the interfacial phases. A conventional TEM (200CX, Jeol, Japan) operated at 200 keV was used to collect electron diffraction data and the smallest area of analysis was equivalent to that of a circle with a diameter of ~500 nm. The camera length was monitored using an Al thin film, which was supplied by Agar Scientific, UK.

The thicknesses of the layers at the braze/alumina interface were measured from SEM images as a function of T_p and τ. Care was taken while making these measurements to take into account variations in the thickness of each reaction layer. The thickness of the Ti_3Cu_3O layer varied significantly because of the angular nature of the particles, the presence of columnar particles, and the dispersed nature of the particles as the layer breaks down and ceases to be a well defined layer. Twenty measurements were made at regions that had approximately uniform reaction layer thicknesses. The thicknesses are represented by a mean value and ± one standard deviation.

3. Results

3.1. Al_2O_3/Cusil ABA/Al_2O_3 joint system

3.1.1. The A99/Cusil ABA interface

The microstructure of the braze joints prepared with Cusil ABA showed considerable evolution with T_p and τ. A collection of BSEIs of A99/Cusil ABA/A99 cross-sections which were prepared using the parameters of 815°C ≤ T_p ≤ 875°C and

2 min ≤ τ ≤ 300 min are shown in Figures 3–5. These images reveal significant changes to the interfaces between alumina and the braze alloy, particularly as a function of τ. Continuous reaction bilayers formed at the interfaces when a short joining time of 2 min was used. At a T_p of 815°C, a thin layer on the alumina, which was typically between 60 and 90 nm in thickness and is referred to as layer 1, formed beside a 0.9–1.3 μm thick layer, which was in contact with the braze alloy and is referred to as layer 2. Occasionally, small quantities of braze alloy were found between layers 1 and 2, and amongst the particles in layer 1, arising from intergranular flow of braze alloy through layer 2, but in general, layers were physically touching. This particular interfacial morphology was also observed in a joint that was held at 900°C for up to 2 min in a vacuum (10^{-4} mbar). In this case, the thicknesses of layer 1 and 2 varied between 50–130 nm and 1.1–2.0 μm respectively. At a τ of 2 min, the thickness of layer 1 increased with T_p in the range 845 – 875°C from 50–100 nm to 60–120 nm, while the width of layer 2 increased from 0.8–1.6 μm to 1.0–1.9 μm.

The thickness of each layer at a T_p of 845°C and τ of 2 min compares well with the observation of Stephens et al. [11] of the interfacial structure at the (0001) sapphire/Ag–34.1Cu–1.7Ti wt% interface, which was held at 845°C for 6 min. Here, the joining configuration used allowed for reactions to occur at only one interface, as opposed to two interfaces, and the maximum bond area was about 1.3×10^{-4} m^2, which agrees with the components used in this work. As a consequence, Stephens et al. [11] observed layers which were approximately twice as wide as those observed in this work.

By lengthening τ to 15 min at 815°C, the quantity of braze alloy found between layer 1 and 2 had increased to cause the layers to separate. The thicknesses of layer 1 and 2 had increased marginally, to 70–110 nm and 0.95–1.3 μm respectively, with this change. Further growth of layer 1 occurred by increasing T_p at a τ of 15 min. In the temperature range of 845–875°C, the thickness of layer 1 had increased from 65–140 nm to 70–185 nm. This also caused the particles in layer 2 to separate from each other to leave a broken layer, along with a clear layer of braze alloy between it and layer 1. A similar interfacial structure was produced with a τ of 30 min, but growth of the particles in layer 1 was more significant. The thickness of this layer varied from ~120 to ~350 nm in the temperature range of 815–875°C. Further increases in τ produced an inhomogeneous interfacial structure across the joint. A structure similar to that observed whilst using a τ of 30 min formed along the majority of the interfaces when τ was increased to 45 min. However, several regions with no reaction products present at the interface were observed. Nevertheless, no voids were observed between the ABA and alumina in these joints. The highest degree of inhomogeneity in the interfacial structure was observed with a τ of 300 min and T_p of 845°C. At this condition, significant decomposition of layer 2 had occurred. In such regions along the interface where this was particularly observable, layer 1 became thicker (up to ~1 μm) and was now the most significant interfacial phase.

The crystal structure and composition of the particles in each layer were identified by a TEM–EDS investigation. A high magnification HAADF image of an A99/Cusil

ABA interface which was held at 815°C for 2 min is shown in Figure 6, along with the corresponding bright field image. Layers 1 and 2 are polycrystalline. EDS analysis revealed Ti and O were major components of layer 1, while Al was a minor component (Figure 6c). The composition of this layer was 49.5Ti–47.3O–2.8Al–0.4Cu at%. The crystal structure of the particles in this layer was identified by electron diffraction as that of γ–TiO (cubic, $Fm\bar{3}m$, space group 225) with a unit cell length of 4.21 Å. A selection of diffraction patterns with low index-zone axes from this phase is shown in Figure 7. There were no clear connections between the composition or the unit cell length of γ–TiO and T_p or τ. EDS analyses consistently and repeatedly suggested a slightly metal-rich titanium oxide formed with ~1 to 4 at% Al as a solute. The lattice parameter of this phase varied between 4.20 to 4.24 Å.

Isolated particles of Ti_3O_2 were also identified in layer 1 at two different A99/Cusil ABA interfaces and a B95/Cusil ABA interface, which were held at the 845°C for 45 or 300 min. A single particle of Ti_3O_2 was observed at each interface as shown in Figure 8. The composition of this phase, as determined by EDS, was 58.2Ti–41.2O–0.4Al–0.2Cu at%. Electron diffraction analysis identified the crystal structure of this phase as that of Ti_3O_2 (hexagonal, P6/*mmm*, space group 191) with lattice parameters of a = 4.99 Å and c = 2.88 Å; a selection of diffraction patterns with low-index zone axes is shown in Figure 9. This particular titanium oxide has been observed on alumina in a recent investigation of a 99.9Al_2O_3/Ag–26.7Cu–4.5Ti wt% interface that was held at 915°C for 20 min [12], though it was not observed alongside any other titanium oxide. The possibility of further titanium oxides forming as very minor components of layer 1, which have been missed by the TEM analysis, has not been discounted because only very small areas of interface were analysed using this technique, due to the necessity for thin, electron transparent samples.

The chemical composition of layer 2 was consistent with that of Ti_3Cu_3O with ~6.5 at% Al as a solute (Figure 6d). A typical composition for this phase was 43.3Ti–38.5Cu–6.5Al–11.7O at% and it was found to vary in a path perpendicular to the interface in approximately half of the samples. The Ti and Cu contents decreased from ~44.5 to ~42.0 at% and ~39.5 to ~37.5 at% respectively from the braze/Ti_3Cu_3O interface to Ti_3Cu_3O/γ–TiO interface. In addition, the Al and O contents increased along the same path from ~6.0 to ~7.5 at% and ~10.5 to ~13.0 at% respectively. These concentration gradients are most likely caused by a variation in the thickness of the samples. The crystal structure was identified by electron diffraction as that of Ti_3Cu_3O (cubic, F$d\bar{3}m$, space group 227) with a unit cell length that varied between 11.2 and 11.4 Å. A selection of diffraction patterns with low index-zone axes from this phase is shown in Figure 10. The absence of h00 reflections, for h = 4n + 2 in the [001] pattern agrees with the diamond-cubic type structure of Ti_3Cu_3O. The 002 reflection appears in the [110] pattern by double diffraction, for which $1\bar{1}1$ and $\bar{1}11$ are simultaneously on the Ewald sphere. No connections between the unit cell length of this phase and T_p or τ were identified.

The residual ABA was composed of two phases. The bright regions in the ABAs shown in Figures 3–5 are Ag-rich and the darker regions are Cu-rich. The

composition of these phases did not change significantly with T_p while τ was in the range of 2 to 45 min. The Ag-rich phases contained 15–25 at% Cu and 10–12 at% Al, while the Cu-rich phases contained a significantly lower quantity of Al, between 1 and 2 at%, and small amounts of Ti, at a level of ~0.5–1.0 at%, within a region of ~8 μm from the ABA/alumina interface. The quantity of Al in each phase was found to decrease slightly with distance from this interface. Substantial decomposition of Ti_3Cu_3O caused by extending τ to 300 min at a T_p of 844°C was accompanied by increases in the Al content for both of these phases at regions close to the ABA/alumina interface. Here, the Ag-rich phase contained ~20 at% Al and ~15 at% Cu, and the Cu-rich phase contained ~3 at% Al and ~0.2 at% Ti. At this condition, ~1 at% Si was also found in the Cu-rich phase near the ABA/B95 interface.

3.1.2. Effect of reducing the purity of alumina on interfacial structure and chemistry – the A95/ and B95/Cusil ABA interfaces

Elements such as Si and Ca were introduced to the interface with the ABA in the form of various oxides by altering the grain boundary microstructure in alumina. BSEIs of the interfacial structures in three joints that were prepared in a vacuum and using the same brazing cycle (T_p of 845°C and τ of 15 min), but with three different grades of alumina, are shown in Figure 11. In each joint, layer 2 has broken and is separated from layer 1, which is continuous across alumina, by braze alloy. The thickness of each layer did not vary significantly by altering the purity of alumina. The thickness was typically between ~60 and ~140 nm for layer 1, and ~1.0 and ~1.6 μm for layer 2. Reducing the purity of alumina did not significantly affect the interfacial structure. This conclusion agrees with the sessile drop work by Voytovych et al. [24].

This behavior was supported by the formation of solid solutions at the interface, where elements from the secondary phase were incorporated into the reaction layers. The HAADF image shown in Figure 12 is an example of a region of interface where braze alloy had flowed between the Al_2O_3 grains to wet an amorphous calcium silicate particle. The distribution of Si and Ca at the interface is shown by the EDS maps of these elements in Figures 12g and 12h. Here, Si was mainly identified in the Ti_3Cu_3O layer at a level of ~5 at%. The Al content was low at ~2 at% and as a result the unit cell length did not change (a = 11.3 Å). However, in general, ~1 at% Si and ~6 at% Al was identified in layer 2 at the B95/ and A95/Cusil ABA interfaces. Ca was mainly found in γ–TiO grains that were dispersed in the Ti_3Cu_3O layer, with a typical composition of 31.5Ti–21.3Ca–45.5O–1.7Al at%. The cubic crystal structure of γ–TiO was maintained with this level of Ca substituting Ti and had a unit cell length of 4.24 Å.

3.1.3. Reactivity and thermal stability of the reaction products at the B95/Cusil ABA interface

A B95/Cusil ABA/B95 joint, which was prepared by holding for 2 min at T_p of 815°C, was heat treated in argon gas for various lengths of time, ranging from 5 h to

150 h, to study further the relative thermal stabilities of the interfacial phases. The images shown in Figure 13 were acquired at high magnification and show the changes that occurred at the interface with time. Between 5 h and 20 h, the Ti_3Cu_3O particle size and total volume decreased with time, while the opposite occurred with the titanium oxide on alumina. Small particles between ~10 and ~200 nm in size containing Ti and O, and therefore likely to be a titanium oxide, were also observed on SEM-EDS chemical maps in the braze alloy amongst the remaining Ti_3Cu_3O particles. No Ti_3Cu_3O was observed after heat treating for 50 h. Ti_3Cu_3O had released its Al content, and a small quantity of O, into the Ag- and Cu-rich phases of the ABA. The Ti and remaining O content supported the growth of titanium oxide on alumina. Isolated particles of Ti_2Si, ~2 μm in size, were also observed on alumina, alongside the titanium oxide particles, after heat treating for 75 h. The majority of the Si content in this titanium silicide is provided by the secondary phase in alumina.

3.2. Al_2O_3/Ticusil/Al_2O_3 joint system

BSEIs of three B95/Ticusil/B95 joints, which were held at 900°C for 2, 15 and 30 min are shown in Figure 14. Layers 1 and 2 were continuous over the length of the joints that were held at T_p for 2 and 15 min. Holding for 2 min produced a very thin layer 1, with a thickness that varied between 5 and 30 nm, and a 2.2 μm thick layer 2. The thickness of layer 1 and 2 increased to ~70 nm and ~2.4 μm respectively with this change to τ. Extending τ to 30 min caused layer 2 to divide and allow braze alloy to flow towards alumina. At the same time significant growth of layer 1 occurred to produce a continuous layer with a thickness that varied between ~230 and ~600 nm. The identity of layers 1 and 2 were determined by a TEM–EDS investigation. Layer 2 was identified as Ti_3Cu_3O, with ~6.5 to ~7.5 at% Al as a solute and a unit cell length of ~11.3 Å. A single phase was observed in layer 1 at these interfaces, which was identified as γ–TiO with a typical chemical composition of 48.9Ti–46.5O–4.1Al–0.5Cu at% and unit cell length of ~4.19 Å.

4. Discussion

4.1. Interfacial reaction products: γ–TiO and Ti_3Cu_3O

The phases identified at the Ag–Cu–Ti/Al_2O_3 interfaces agree with the majority of the studies summarised in Table 1, i.e. a thin layer of TiO next to the alumina, and a thicker layer of M_6O between this and the body of the braze.

The thin layer on alumina was mainly composed of γ–TiO grains. Small quantities of Ti_3O_2 were also observed in this layer, but far less frequently and in singular grain form. It is not unusual to have small quantities of another titanium oxide nucleate during synthesis of γ–TiO [28], because this phase is not a state of thermodynamic equilibrium at temperatures below ~1250°C [29]. At such temperatures, phase transitions leading to a variety of ordered states can occur. The detection of γ–TiO

contradicts the Ti–O phase diagram [29], even when a simplified γ–TiO phase region that excludes many of the ordered states is considered, as described in other assessments of the Ti–O phase diagram [30,31]. In such cases, γ–TiO may be expected to decompose in to α–TiO and Ti_2O_3 at temperatures below ~450°C. The retention of γ–TiO during cooling from T_p is attributed to the cooling rates used, which were high enough to avoid any significant atomic rearrangement and ordering of the crystal structure, and further transformations. Valeeva et al. [32] showed by selecting a very slow cooling rate of 10°C h^{-1} α–TiO can be prepared from γ–TiO, which was annealed at ~1060°C for 3 h. Such a low rate of cooling is not used while brazing because it is impractical. In the brazing process, the cooling rate is typically between 10 and 20°C min^{-1}, and therefore γ–TiO is kinetically limited in transforming to equilibrium phases, so it is observed as a metastable phase in brazed joints.

γ–TiO is homogeneous over a wide range from about $TiO_{0.7}$ to $TiO_{1.25}$. Anderson et al. [33] observed that the unit cell length of γ–TiO decreased linearly with oxygen content in this range, varying from ~4.20 to ~4.17 Å. Near-equiatomic titanium monoxide $TiO_{0.995}$ was found to have a unit cell length of 4.18 Å, which is in agreement with more recent reports [32,34]. On this criterion, the γ–TiO grains in the brazed joints would be Ti-rich, since the unit cell length varied between 4.19 and 4.24 Å. The formation of non-stoichiometric and metal-rich γ–TiO would also be consistent with the EDS data. However, taking into account the difficulties in determining the relative amounts of Ti and O by EDS, it has not been established with absolute confidence that oxygen is present in the γ–TiO grains in non-stoichiometric amounts.

Ti_3Cu_3O has been identified as the main product of the reactions between the ABAs and alumina. A mixture of equiaxed and columnar grains of this phase with up to ~7.5 at% Al were observed at each interface. Kelkar and Carim [35] reported that Ti_3Cu_3O likely accommodates Al by substituting Cu. In the joints prepared with 95.0 wt% Al_2O_3, Si was also identified as a solute, nonetheless a total of up to ~7 at% solute was observed. It is likely that Si and Al form solid solutions with Ti_3Cu_3O (i.e. $Ti_3(Cu+Al+Si)_3O$) by the same mechanism because their levels fluctuated in a coordinated manner. At regions close to a secondary phase in alumina, the Si content in Ti_3Cu_3O was relatively high, at a level of ~5 at%, and the Al content was lower, at ~2 at%. Further away from the impurity, the Si content fell to ~1 at% and the Al content increased to ~6 at%. The typical amount of Si in Ti_3Cu_3O was found to be low, at ~1 at%, and therefore is not expected to significantly affect the mechanical properties of the oxide.

The thermal expansion mismatch between the braze and alumina can generate residual stresses in the joints on cooling from T_p. The braze alloy is expected to help mitigate the mismatch in the coefficients of thermal expansion (CTE) by stress relaxation or creep deformation processes. High dislocation densities were observed in the Ag-rich and Cu-rich regions of the braze. The distribution of the dislocations in the phases was complex and their characteristics were not determined in this study. Very few dislocations were observed in Ti_3Cu_3O. The observations of Kelkar and

Carim [36] of various mechanical, thermal and electrical properties of bulk Ti_3Cu_3O suggest that there are gradual transitions across the braze/alumina interface in terms of these properties. The values of the CTE and elastic modulus for Ti_3Cu_3O were found to be between those of alumina and metals such as Cu and Ag. However, the structural characteristics of this compound suggest that it would be difficult to dissipate residual stresses at the interfaces. Carim and Mohr [37] attributed low flexural strengths obtained by four–point bend testing for $Al_2O_3/Ti_3Cu_3O/Al_2O_3$ joints that were held at 1290°C for 40 minutes to a lack of ductility in the Ti_3Cu_3O interlayer. The flexural strength values were not given, but it was stated that they were approximately an order of magnitude lower than the strength obtained for a joint prepared with a commercially available Ag–Cu–Ti alloy.

No definitive orientation relationships could be identified between the particles in the Ti_3Cu_3O or γ–TiO layer and alumina to support an argument for strain energy minimisation across the interface by spatial ordering of the reaction layers. This is consistent with the observations of Ichimori et al. [25] of the reaction bilayers formed between various orientations of sapphire and Ag–28.4Cu–4.9Ti wt% during a brazing cycle that peaked at 900°C for 5 min.

The value for electrical resistivity of bulk Ti_3Cu_3O (5×10^{-6} Ω m) reported by Kelkar and Carim [36] is also intermediate between those of alumina (~10^{14} Ω m) and metals such as Ag and Cu (~10^{-8} Ω m), but it is clearly much closer to those of the metals. This suggests Ti_3Cu_3O has some metallic character and could provide a less abrupt change in chemical bonding across the interface. Voytovych et al. [24] showed that successful wetting of sapphire by Ag–Cu–Ti alloys is dependent on the formation of compounds such as Ti_3Cu_3O and they have attributed this to the metallic nature of the Ti_3Cu_3O-type compounds. In a series of sessile drop experiments, three different Ag–Cu–Ti alloys with various titanium content, 0.7, 2.9 and 8.0 at% Ti, were used to wet sapphire at 900°C, and the contact angles obtained after 30 minutes were recorded alongside the interfacial reaction products. The TiO–Ti_3Cu_3O bilayer structure normally observed at the Ag–Cu–Ti/Al_2O_3 interface only appeared using the 2.9 at% Ti alloy. The contact angle recorded with this Ti content was 10°. Higher or lower Ti contents resulted in the formation of a single reaction layer. With the 0.7 at% Ti alloy, wetting was controlled by a titanium oxide layer, resulting in a contact angle of 63°. With the 8.0 at% Ti alloy, a layer containing both Ti_3Cu_3O and Ti_4Cu_2O was observed, resulting in a similar contact angle to that obtained with the 2.9 at% Ti alloy. The electrical resistivity appears to be independent of the Ti/Cu ratio [36], so the wetting characteristics of these M_6O compounds should be identical. In other words, the formation of either M_6O compound should be equally beneficial for wetting.

4.2. Microstructural developments with T_p and τ

The shortest brazing time of 2 min was used at the liquidus temperatures of the ABAs to determine the state of the reaction layers in an early stage after their evolution. At these conditions, the amounts of active element in the ABAs were almost depleted,

primarily by the chemical reaction to form the micrometre-size Ti_3Cu_3O layer. At this stage, the width of the γ–TiO layer on the alumina was less than an order of magnitude lower, and layers were continuous and typically in contact with each other across the joint. At the Cusil ABA/alumina interface, the effects of altering T_p on the structure of the layers were not as prominent as those caused by altering τ. At a fixed τ, the thickness of the γ–TiO layer and the variation in this measurement across the joints increased with T_p. The width of the Ti_3Cu_3O layer also increased with T_p at a τ of 2 min (i.e. while this layer remained continuous across the joint).

Additional A99/Cusil ABA/A99 joints were prepared in argon at a T_p of 815°C with τ ranging from 2 – 12 min to study further the effect of τ on the thickness of the interfacial reaction layers. The bilayer microstructures in these joints were very similar and only showed small variations in the thickness of the layers. These are shown as a function of τ in Figure 15. Between 2 and 15 min, there appears to be a trend of longer joining times resulting in slightly thicker layers. Diffusion-controlled growth of the layers has been considered for this range of τ, but a relationship cannot be established conclusively because of the magnitude of the errors associated with the data. The thickness of the γ–TiO layer increases more rapidly with τ beyond 15 min for two reasons. Firstly, an extension of the joining time initially causes the Ti_3Cu_3O layer to dissociate from the γ–TiO layer and then divide to leave a broken layer of Ti_3Cu_3O. This degradation process of the Ti_3Cu_3O enables intergranular flow of braze through the Ti_3Cu_3O layer, transporting any available active element closer to the reaction front to enable further growth of the γ–TiO layer. Such a structure was observed at a T_p of 815°C by holding for 30 min; this holding time reduced to 15 min as T_p was increased. Secondly, the Ti_3Cu_3O particles themselves decompose chemically during the longer joining times so that most of the Ti and O content is redistributed by growth of γ–TiO particles.

Increasing T_p and τ eventually forms inhomogeneous interfacial structures, with some regions of interface lacking evidence for preserving a chemical bond between the ABA and alumina. Other regions show significant development of the titanium oxide layer along with decomposition of the Ti_3Cu_3O layer. This was also apparent during the heat treatment of a B95/Cusil ABA/B95 joint at 815°C for lengths of time up to 150 h, which indicated that the Ti_3Cu_3O phase was less stable than the titanium oxide on alumina at this temperature.

4.3. Reaction bilayer formation process

Both Cusil ABA and Ticusil have been shown to react with alumina to produce Ti_3Cu_3O and γ–TiO in significant quantities, with the Ti_3Cu_3O phase being by far the main product of the reaction processes occurring at the Ag–Cu–Ti/Al_2O_3 interfaces. It is anticipated that Ti and Cu diffuse rapidly to alumina on melting the ABA initially to form M_6O by the schematic reaction:

$$Al_2O_3 + 9\ Ti + 7\ Cu \longrightarrow Ti_9Cu_7Al_2O_3 \qquad [1]$$

where the maximum solubility of Al in Ti_3Cu_3O is limited to ~9.5 at% if this element is accommodated in the oxide by only substituting Cu, as described by Kelkar and Carim [35]. In the brazed joints, only ~6.5 at% Al was identified in the M_6O phase. However, Al was also found to form solid solutions with the phases in the ABA, in particular with Ag, at regions close to the ABA/alumina interface. If the formation of these solid solutions is put aside for simplicity, the thermodynamic feasibility of Ti_3Cu_3O formation as described in equation 1 can then be assessed using the reaction free energy

$$\Delta G_1 = G_{Ti_3Cu_3O} + \frac{2}{3} G_{Al} - \frac{1}{3} G_{Al_2O_3} - 3\, G_{Ti} - 3\, G_{Cu} \qquad [2]$$

where G is the Gibbs free energy from the work of Barin [38]. Using the value of ΔG_1 estimated by Kelkar et al. [39] at 945°C, which was approximately –511 kJ mol^{-1}, $G_{Ti_3Cu_3O}$ is estimated to be approximately –1 MJ mol^{-1} at this temperature. As no further thermochemical information on Ti_3Cu_3O could be found, it was assumed as a first approximation that this estimate was sufficiently independent of temperature within experimental error for this to be a reasonable estimate at 815–875°C. Consequently, at 1100 K, ΔG_1 is negative and approximately –123 kJ mol^{-1}. According to this estimation, equation 1 would be favoured thermodynamically at temperatures above the liquidus temperature of the ABA.

On the formation of a Ti_3Cu_3O layer, it is suggested that Ti diffuses through the layer more rapidly than Cu, and it then reacts with alumina to form titanium oxide by the schematic reaction:

$$3x\ Ti + y\ Al_2O_3 \longrightarrow 3\ Ti_xO_y + 2y\ Al \qquad [3]$$

where a proportion of Al forms a solid solution with the titanium oxide. The evidence of thinner titanium oxide layers forming at interfaces where there are wider Ti_3Cu_3O layers supports this. For example, joining B95 with Cusil ABA at the liquidus temperature of the alloy (815°C) for 2 min formed 60 to 90 nm thick γ–TiO and ~1 μm thick Ti_3Cu_3O layers. Joining this ceramic with Ticusil for the same length of time at a higher liquidus temperature of 900°C formed a Ti_3Cu_3O layer that was approximately twice as thick and a thinner γ–TiO layer, which had a width between 5 and 30 nm. On dividing the Ti_3Cu_3O layer, intergranular diffusion of Ti could then occur to result in an increase in the growth rate of the titanium oxide layer. The titanium oxide layer is usually observed to be relatively thin because most of the active element has already been consumed by the primary reaction to form Ti_3Cu_3O and τ is normally lower than 30 min, i.e., significant thermal degradation of Ti_3Cu_3O, which supports further growth of the titanium oxide layer, does not occur.

5. Conclusions

Two Ag–Cu–Ti based ABAs (Ag–35.3Cu–1.8Ti and Ag–26.7Cu–4.5Ti wt%) have been used to join different grades of alumina to themselves at various conditions by producing a typical interfacial structure of Ag–Cu alloy /Ti_3Cu_3O/γ−TiO/Al_2O_3. The ternary oxide is the main product of the reactions between the ABAs and alumina. Considerable evolution of the interfacial structure in the joints prepared with Ag–35.3Cu–1.8Ti wt% was observed, particularly as a function of joining time. At times shorter than 30 min, the Ti_3Cu_3O layer dissociated from the γ−TiO layer and then divided, but the interfacial structure remained approximately uniform across the joints. Extended joining times produced interfacial structures that varied considerably over short distances across the length of the joints. Heat treatments at 815°C indicated that Ti_3Cu_3O is not stable at this temperature with respect to titanium oxide.

It has been shown that elements such as Si and Ca from the secondary phases in alumina can form solid solutions with the interfacial phases and as a result they do not have a significant effect on the overall interfacial structure. Si was mainly identified in Ti_3Cu_3O and Ca in γ−TiO.

Based on the experimental results, a reaction mechanism has been provided to suggest that Ti_3Cu_3O forms initially at temperatures above the liquidus temperature of ABA.

Acknowledgements

We acknowledge the financial support for this study provided by AWE and are grateful to Dr T.R. Barnes and J. Newman of AWE for vacuum furnace brazing of components, and Iris Buisman of the Department of Earth Sciences at the University of Cambridge for assistance with electron microprobe analysis of alumina substrates.

References

[1] E. Dörre, H. Hübner, Alumina: processing, properties, and applications, Springer Berlin Heidelberg, Berlin, 2011.

[2] R.W. Messler, Joining of advanced materials, Butterworth-Heinemann, Massachusetts, 1993.

[3] J.A. Fernie, R.A.L. Drew, K.M. Knowles, Joining of engineering ceramics, Int. Mater. Rev. 54 (2009) 283-331.

[4] H.J. Nolte, Metalized ceramic, US Patent 2667432, 1954.

[5] A.W. Hey, Metallizing ceramic surfaces, in: M.G. Nicholas (Ed.), Joining of Ceramics, Chapman & Hall, London, 1990, pp. 56-72.

[6] K.M. Jasim, F.A. Hashim, R.H. Yousif, R.D. Rawlings, A.R. Boccaccini, Actively brazed alumina to alumina joints using CuTi, CuZr and eutectic AgCuTi filler alloys, Ceram. Int. 36 (2010) 2287-2295.

[7] Y.C. Yoo, J.H. Kim, K.Park, Microstructural characterisation of Al_2O_3/AISI 8650 steel joint brazed with Ag-Cu-Sn-Zr, Mater. Lett. 42 (2000) 362-366.

[8] R.E. Loehman, A.P. Tomsia, Reactions of Ti and Zr with AlN and Al_2O_3, Acta Metall. Mater. 40 (1992) S75-S83.

[9] R.E. Loehman, F.M. Hosking, B. Gauntt, P.G. Kotula, Reactions of Hf-Ag and Zr-Ag alloys with Al_2O_3 at elevated temperatures, J. Mater. Sci. 40 (2005) 2319-2324.

[10] S. Hahn, M. Kim, S. Kang, A study of the reliability of brazed Al_2O_3 joint systems, IEEE Trans. Compon. Packag. Manufac. Technol. Part C. 21 (1998), 211-216.

[11] J.J. Stephens, F.M. Hosking, T.J. Headley, P.F. Hlava, F.G. Host, Reaction layers and mechanisms for a Ti-activated braze on sapphire, Metall. Mater. Trans. A. 34 (2003) 2963-2972.

[12] K-L. Lin, M. Singh, R. Asthana, Interfacial characterization of alumina-to-alumina joints fabricated using silver-copper-titanium interlayers, Mater. Charact. 90 (2014), 40-51.

[13] D. Janickovic, P. Sebo, P. Duhaj, P. Svec, The rapidly quenched Ag-Cu-Ti ribbons for active joining of ceramics, Mater. Sci. Eng. A. 304-306 (2001) 569–573.

[14] H. Hongqi, W. Yonglan, J. Zhihao, W. Xiaotian, Interfacial reaction of alumina with Ag-Cu-Ti alloy, J. Mater. Sci. 30 (1995) 1233-1239.

[15] S. Suenaga, M. Nakahashi, M. Maruyama, T. Fukasawa, Interfacial reactions between sapphire and silver-copper-titanium thin film filler metal, J. Am. Ceram. Soc. 80 (1997) 439-444.

[16] W. Byun, H. Kim, Variations of phases and microstructure of reaction products in the interface of Al_2O_3/Ag–Cu–Ti joint system with heat-treatment, Scr. Metall. Mater. 31 (1994) 1543-1547.

[17] P.T. Vianco, J.J. Stephens, P.F. Hlava and C.A. Walker, Titanium scavenging in Ag-Cu-Ti active braze joints, Weld. J. 82 (2003), 268-S-277-S.

[18] C. Valette, M.F. Devismes, R. Voytovych, N. Eustathopoulos, Interfacial reactions in alumina/CuAgTi braze/CuNi system, Scr. Mater. 52 (2005) 1-6.

[19] A.H. Carim, Convergent-beam electron diffraction "fingerprinting" of M_6X phases at brazed ceramic joints, Scr. Metall. Mater. 25 (1991) 51-54.

[20] M.L. Santella, J.A. Horton, J.J. Pak, Microstructure of alumina brazed with a silver-copper-titanium alloy, J. Am. Ceram. Soc. 73 (1990) 1785-1787.

[21] A. Kar, S. Mandal, R.N. Ghosh, T.K. Ghosh, A.K. Ray, Role of Ti diffusion on the formation of phases in the Al_2O_3-Al_2O_3 brazed interface, J. Mater. Sci. 42 (2007) 5556-5561.

[22] S. Mandal, A.K. Ray, A.K. Ray, Correlation between the mechanical properties and the microstructural behaviour of Al_2O_3-(Ag-Cu-Ti) brazed joints, Mater. Sci. Eng. A. 383 (2004), 235-244.

[23] W.C. Lee, O.Y. Kwon, C.S. Kang, Microstructural characterization of interfacial reaction products between alumina and braze alloy, J. Mater. Sci. 30 (1995), 1679-1688.

[24] R. Voytovych, F. Robaut, N. Eustathopoulos, The relation between wetting and interfacial chemistry in the CuAgTi/alumina system, Acta Mater. 54 (2006) 2205-2214.

[25] T. Ichimori, C. Iwamoto, S. Tanaka, Nanoscopic analysis of a Ag-Cu-Ti/sapphire brazed interface, Mater. Sci. Forum. 294-296 (1999) 337-340.

[26] American Society for Testing and Materials (ASTM), Annual book of ASTM standards 1996, Standard test method for tension and vacuum testing metallized ceramics seals, vol. 10.04, ASTM International, USA, 1996.

[27] L.A. Giannuzzi, F.A. Stevie, A review of focussed ion beam milling techniques for TEM specimen preparation, Micron. 30 (1999) 197-204.

[28] A.A. Valeeva, A.A. Rempel', A.I. Gusev, Electrical conductivity and magnetic susceptibility of titanium monoxide, JETP Lett. 73 (2001) 621-625.

[29] J.L. Murray, H.A. Wriedt, The O-Ti (oxygen-titanium) system, J. Phase Equilib. 8 (1987) 148-165.

[30] H. Okamoto, O-Ti (oxygen-titanium), J. Phase Equilib. Diff. 32 (2011) 473-474.

[31] P. Waldner, G. Eriksson, Thermodynamic modelling of the system titanium-oxygen, Calphad. 23 (1999) 189-218.

[32] A.A. Valeeva, A.A. Rempel', A.I. Gusev, Two-sublattice ordering in titanium monoxide', JETP Lett. 71 (2000) 460-464.

[33] S. Andersson, B. Collen, U. Kuylenstierna, A. Magneli, Phase analysis studies on the titanium-oxygen system, Acta Chem. Scand. 11 (1957) 1641-1652.

[34] A.I. Gusev, Disorder and long-range order in non-stoichiometric interstitial compounds, Phys. Status Solidi B. 163 (1991) 17-54.

[35] G.P. Kelkar, A.H. Carim, Al solubility in M_6X compounds in the Ti-Cu-O system, Mater Lett. 23 (1995) 231-235.

[36] G.P. Kelkar, A.H. Carim, Synthesis, properties, and ternary phase stability of M_6X compounds in the Ti–Cu–O system, J. Am. Ceram. Soc. 76 (1993) 1815-1820.

[37] A.H. Carim and C.H. Mohr, Brazing of alumina with Ti_4Cu_2O and Ti_3Cu_3O interlayers, Mater. Lett. 33 (1997) 195-199.

[38] I. Barin, Thermodynamic data of pure substances, third ed., VCH Verlagsgesellschaft mbH, Weinheim, 1995.

[39] G.P. Kelkar, K.E. Spear, A.H. Carim, Thermodynamic evaluation of reaction products and layering in brazed alumina joints, J. Mater. Res. 9 (1994) 2244-2250.

Figure captions

Figure 1. BSEIs of a) Cusil ABA and b) Ticusil cross-sections.

Figure 2. Schematic cross-section of the sandwich joining configuration used.

Figure 3. BSEIs of A99/Cusil ABA/A99 cross-sections which were held at 815°C for 2 to 45 min.

Figure 4. BSEIs of A99/Cusil ABA/A99 cross-sections which were held at 845°C for 2 to 300 min.

Figure 5. BSEIs of A99/Cusil ABA/A99 cross-sections which were held at 875°C for 2 to 45 min.

Figure 6. a) HAADF and b) bright-field images of a A99/Cusil ABA interface that was held at 815°C for 2 min, along with EDS spectra from c) γ−TiO and d) Ti_3Cu_3O.

Figure 7. Electron diffraction patterns from γ–TiO with the zone axes a) [110], b) [130] and c) [100].

Figure 8. Single grain of Ti_3O_2 at a A99/Cusil ABA interface that was held at 845°C for 300 min.

Figure 9. Electron diffraction patterns from Ti_3O_2 with the zone axes a) [010], b) [011] and c) [012].

Figure 10. Electron diffraction patterns from Ti_3Cu_3O with the zone axes a) [001] and b) [110].

Figure 11. Reaction layers at the Cusil ABA/Al_2O_3 interface after heating to 845°C and holding for 15 min using ceramics a) A99, b) A95 and c) B95.

Figure 12. a) HAADF image of a region of Cusil ABA/B95 interface where the ABA has wet and reacted with a calcium silicate glassy phase; the interface was held at 845°C for 15 min. The distributions of Ag, Cu, Ti, Al, O, Si and Ca are given in their X-ray maps (b-h).

Figure 13. a) BSEI of a Cusil ABA/B95 interface prepared at 815°C for 2 min and cross-sections of this joint after heat to 815°C in Ar gas and holding for b) 5 h, c) 10 h, d) 20 h, e) 50 h, f) 75 h, g) 100 h and h) 150 h.

Figure 14. Reaction layers at the Ticusil/B95 interface after holding at 900°C for a) 2 min, b) 15 min and c) 30 min.

Figure 15. Thicknesses of the a) γ−TiO and b) Ti_3Cu_3O layers at a T_p of 815°C as a function of τ.

Al_2O_3/Ag–Cu–Ti interface (wt%)	Joining conditions		Interfacial reaction product(s)		Method [a]	Ref.
	T_p (°C)	τ (min)	Phase	Thickness (μm)		
>96.0%Al_2O_3/Ag–33.5Cu–1.5Ti	830	10	$TiO_{1.04}$ Ti_4Cu_2O	– –	TEM EDS WDS EPMA	[10]
99.0%Al_2O_3/Ag–28.1Cu–1.5Ti	950 – 1100	1 – 10	δ–TiO (only at 950°C) α–TiO Ti_3Cu_3O	– – –	XRD EDS AES	[16]
Al_2O_3/Ag–35.1Cu–1.6Ti	850	5	Ti_xO_y	1.5 – 2.3	OM	[17]
(0001) Sapphire/Ag–34.1Cu–1.7Ti	845	6	γ–TiO Ti_2O [b] Ti_3Cu_3O	0.02 – 0.2 – ~2.2	TEM EDS EPMA AES	[11]
99.5%Al_2O_3/Ag–36.1Cu–1.8Ti	900	15	$Ti_3(Cu+Al)_3O$	2 – 3	EDS-SEM	[18]
Al_2O_3/Ag–44.8Cu–1.8Ti	950	15	γ–TiO Cu_2O Ti_2O_3	–	TEM EDS-SEM	[13]
Sapphire/Ag–35.0Cu–2.0Ti	825	10	$(Ti+Cu+Al)_6O$	>1	TEM EDS EELS	[19]
Al_2O_3/Ag–36.0Cu–6.0Sn–2.0Ti	900	20	γ–TiO $Ti_3(Cu+Al+Sn)_3O$	0.1 – 0.2 ~3.0	TEM EDS	[20]
99.5%Al_2O_3/Ag–26.8Cu–2.9Ti	800 – 1200	15	γ–TiO Ti_3Cu_3O	–	TEM EPMA	[21]
Al_2O_3/Ag–27.2Cu–3.0Ti Al_2O_3/Ag–38.8Cu–3.0Ti	800 – 1200	15	γ–TiO Ti_3Cu_3O	1.5 – 2.4 3.2 – 5.5	XRD EDS	[22]

Al_2O_3/Ag–48.5Cu–3.0Ti Al_2O_3/Ag–67.9Cu–3.0Ti					EPMA	
99.9%Al_2O_3/Ag–48.1Cu–3.8Ti	920	20	$TiO_{1\pm x}$ (x = 0. 1) Ti_4Cu_2O	~1.2 ~2.4	XRD EDS AES	[23]
Al_2O_3/Ag–17.9Cu–4.2Ti	900	30	Ti_3Cu_3O and Ti_4Cu_2O	3.0 – 5.0	EDS	[24]
99.9%Al_2O_3/Ag–26.7Cu–4.5Ti	915	20	Ti_3O_2 (designated Ti_2O) Ti_3Cu_3O	0.6 – 1.2 5.4 – 6.3	TEM EDS	[12]
99.9% Sapphire/Ag–28.4Cu–4.9Ti	900	5	γ–TiO Ti_3Cu_3O [c]	0.01 – 0.05 1.0 – 2.0	TEM EDS EELS	[25]
99.9%Al_2O_3/Ag–38.0Cu–5.0Ti	800 – 850 900 – 1050	0 – 60 [d]	AlTi Ti_4Cu_2O TiO and Ti_2O $CuTi_2$	[e]	XRD	[14]
99.8%Al_2O_3/Ag–27.0Cu–5.0Ti	980	5 – 90	$(Ti+Al)_4Cu_2O$	–	XRD	[6]

Table 1. Reaction products observed at Ag–Cu–Ti thin foil/Al_2O_3 interfaces, which have been prepared in vacuum or with inert gases. [a]TEM includes techniques such as selected area diffraction and convergent-beam electron diffraction; XRD includes the technique of glancing angle-XRD, optical microscopy (OM), wavelength-dispersive X-ray spectroscopy (WDS), electron probe microanalysis (EPMA), Auger electron spectroscopy (AES) and electron energy loss spectroscopy (EELS). [b]Isolated Ti_2O particles were observed between the γ–TiO and Ti_3Cu_3O layers. [c]Most frequently observed microstructure. Isolated particles of Ti_2O were observed in the γ–TiO layer, along with isolated areas of Ti_3Cu_3O without TiO and occasionally a reaction phase without Ti, that is a Cu-Al-O phase. [d]30 min for 800–1050°C and 0–60 min for 850°C were used. [e]The total reaction layer thickness was found to vary significantly with T_p and τ.

	Al	O	Si	Na	Mg	Ca	Fe	Zr
A99	55.4 ±1.3	44.0 ±1.5	0.2 ±0.1	0.0	0.3 ±0.1	0.0	0.1 ±0.04	0.0
A95	52.2 ±1.9	43.5 ±1.6	2.5 ±0.4	0.3 ±0.1	0.4 ±0.2	0.6 ±0.2	0.2 ±0.1	0.3 ±0.1
B95	52.3 ±1.5	43.2 ±1.9	1.9 ±0.3	0.1 ±0.06	0.4 ±0.2	1.9 ±0.2	0.2 ±0.1	0.0

Table 2. Chemical composition of alumina A99, A95 and B95. Average values from 30 electron microprobe measurements with errors of ± one standard deviation are reported.

	815°C	845°C	875°C
2 min	10^{-6} to 10^{-5} mbar Vacuum*	10^{-8} to 10^{-7} mbar Vacuum	10^{-8} to 10^{-7} mbar Vacuum
15 min	10^{-8} to 10^{-7} mbar Vacuum	10^{-6} to 10^{-5} mbar Vacuum*	10^{-8} to 10^{-7} mbar Vacuum
30 min	Argon	Argon	10^{-8} to 10^{-7} mbar Vacuum
45 min	Argon	10^{-6} to 10^{-5} mbar Vacuum	10^{-8} to 10^{-7} mbar Vacuum
300 min	–	10^{-6} to 10^{-5} mbar Vacuum	–

Table 3. T_p, τ, and the joining environments used to join A99 and B95 to themselves using Cusil ABA. *These conditions were also used to join A95 to itself.

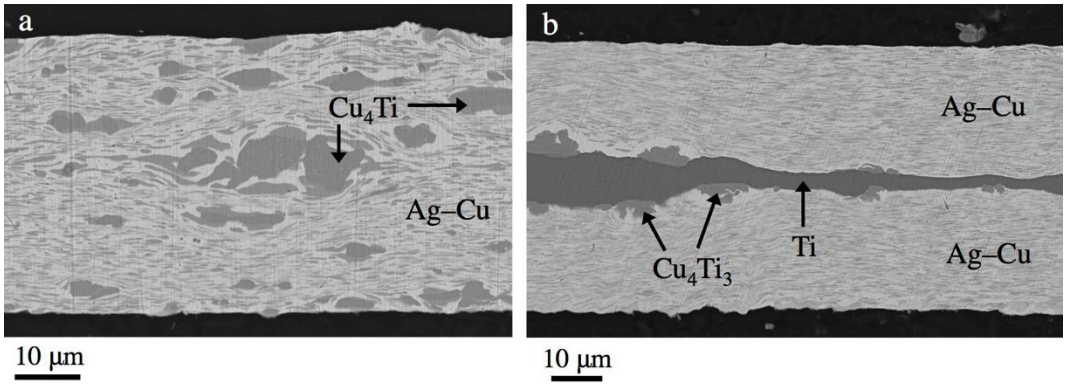

Figure 1. BSEIs of a) Cusil ABA and b) Ticusil cross-sections.

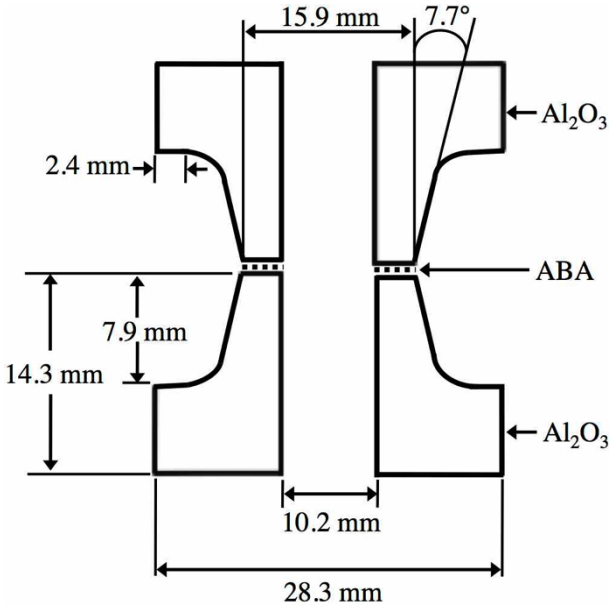

Figure 2. Schematic cross-section of the sandwich joining configuration used.

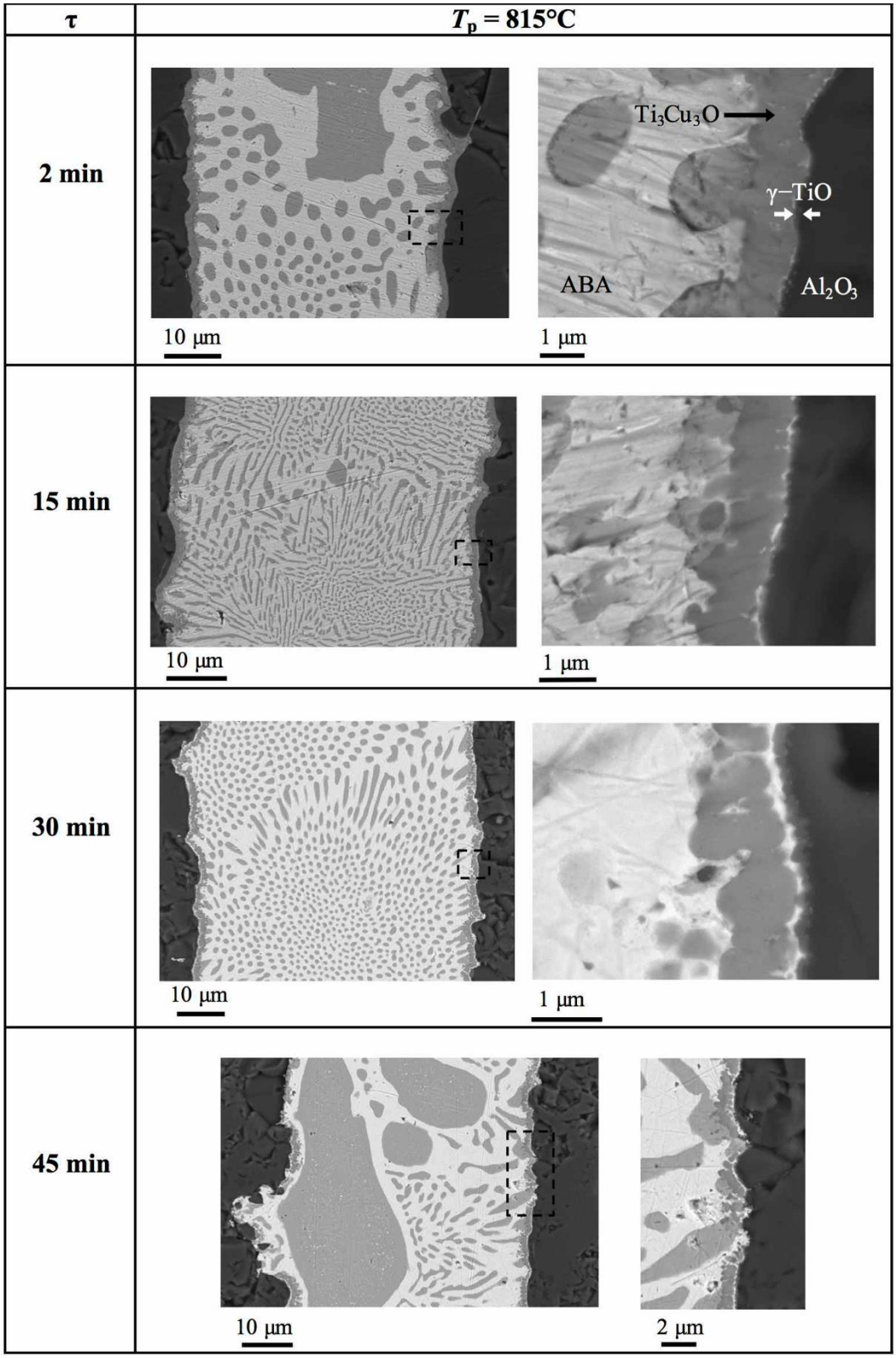

Figure 3. BSEIs of A99/Cusil ABA/A99 cross sections which were held at 815°C for 2 to 45 min.

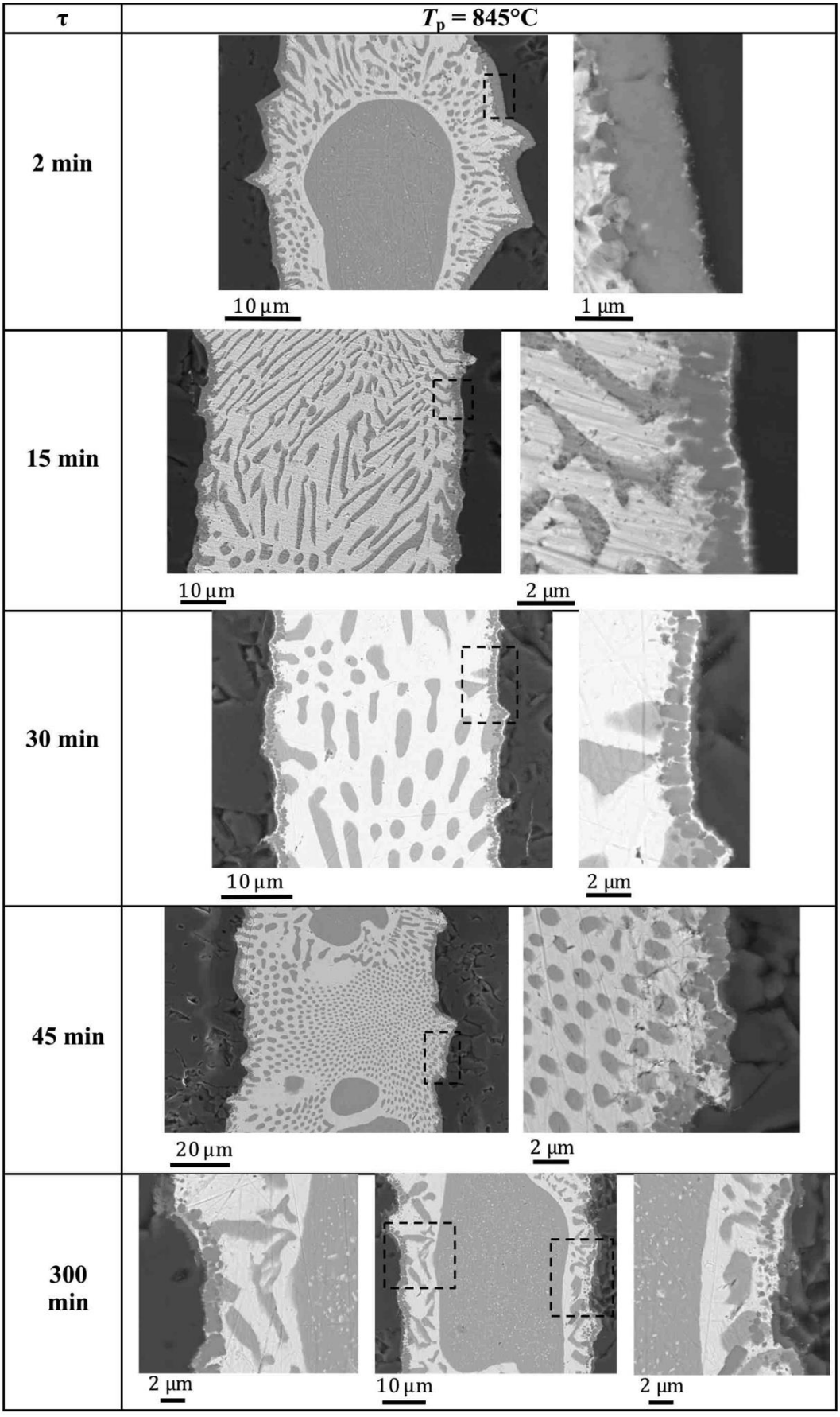

Figure 4. BSEIs of A99/Cusil ABA/A99 cross-sections which were held at 845°C for 2 to 300 min.

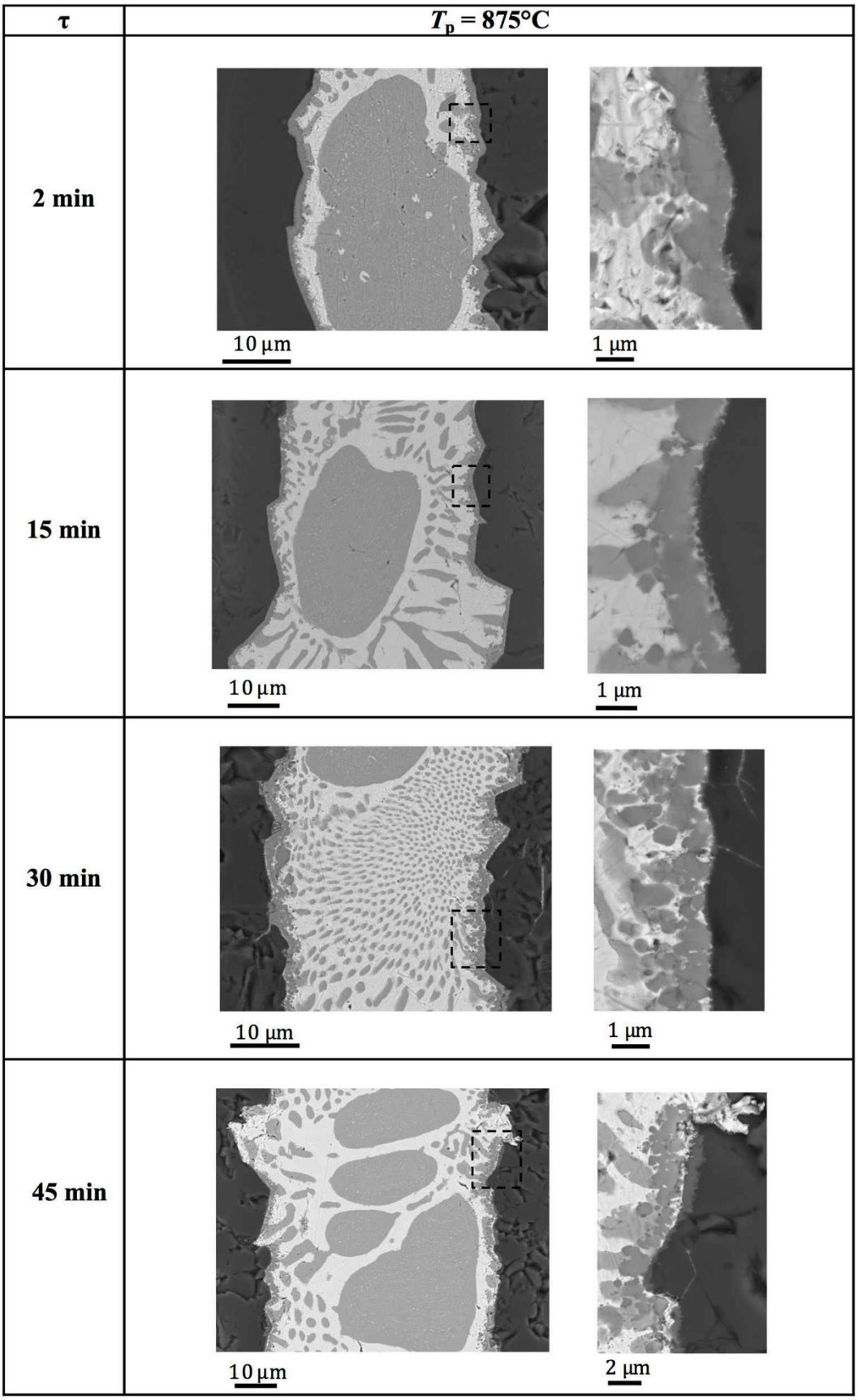

Figure 5. BSEIs of A99/Cusil ABA/A99 cross-sections which were held at 875°C for 2 to 45 min.

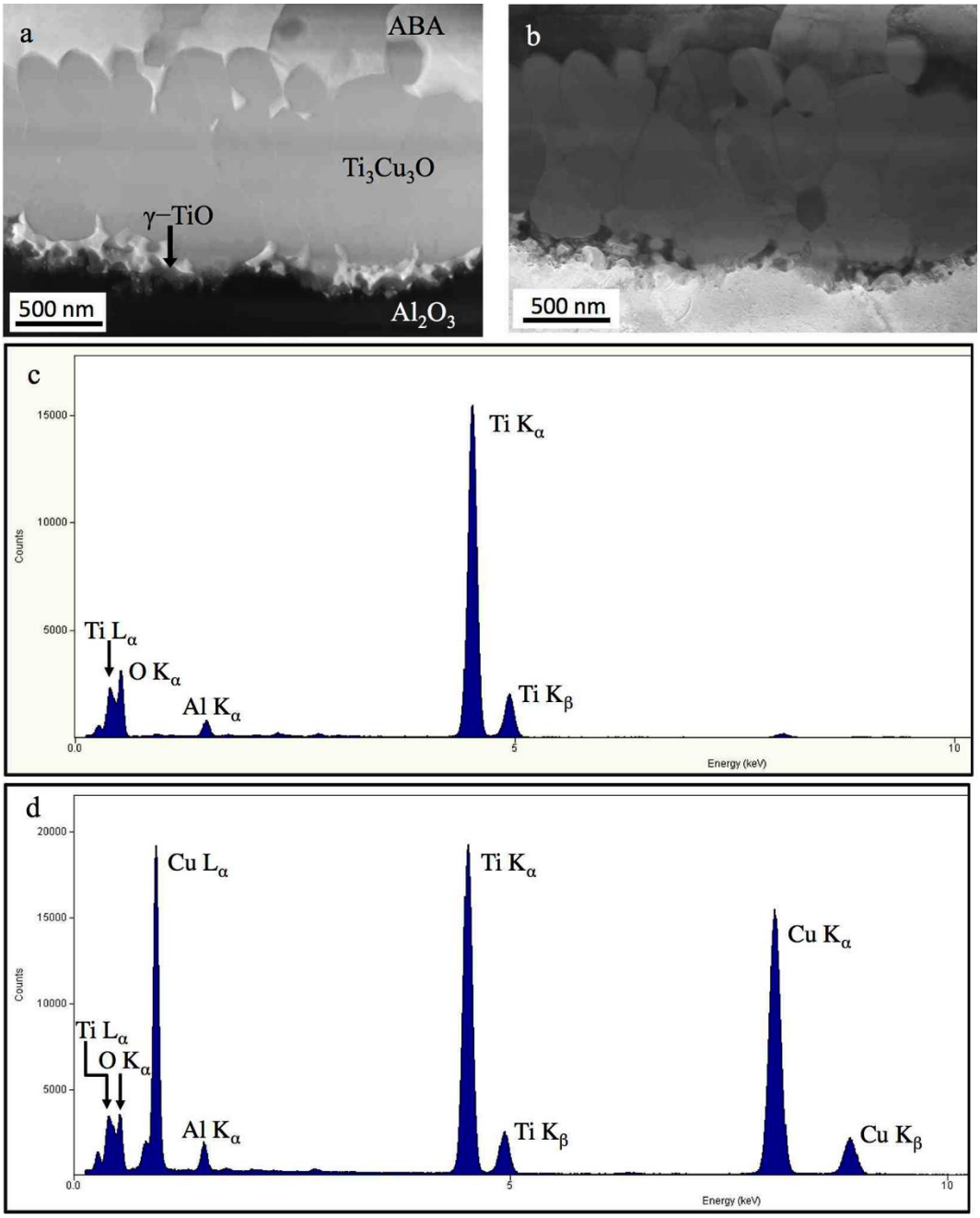

Figure 6. a) HAADF and b) bright-field images of a A99/Cusil ABA interface that was held at 815°C for 2 min, along with EDS spectra from c) γ–TiO and d) Ti_3Cu_3O.

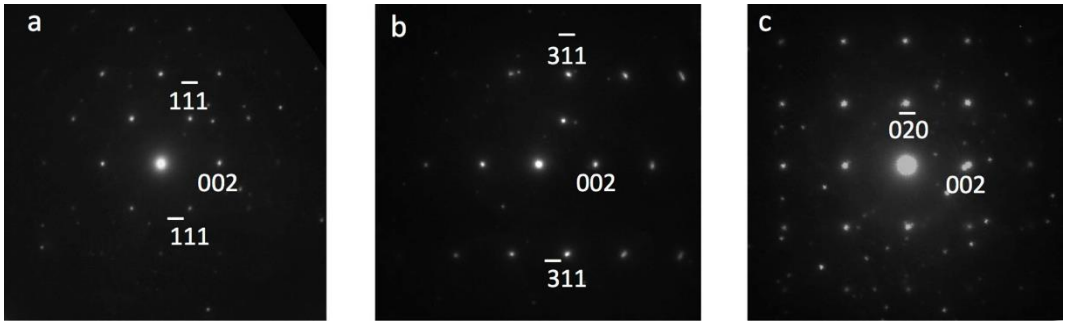

Figure 7. Electron diffraction patterns from γ–TiO with the zone axes a) [110], b) [130] and c) [100].

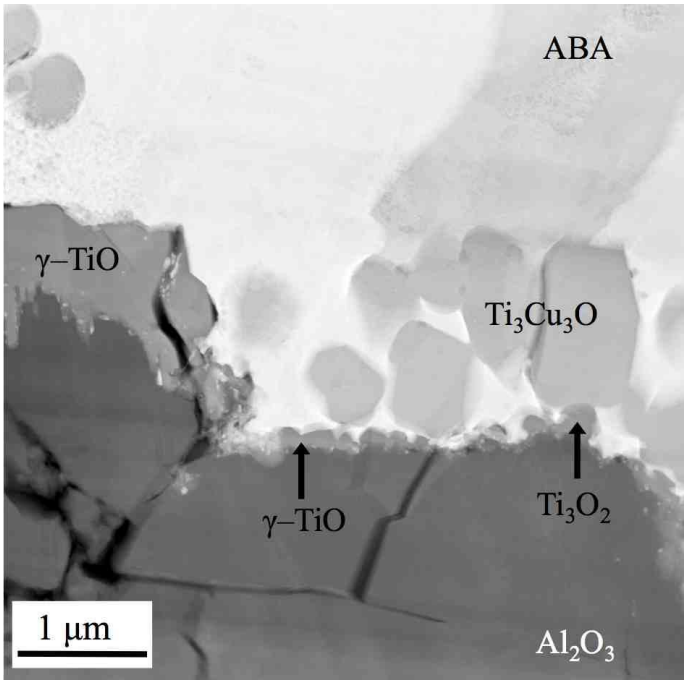

Figure 8. Single grain of Ti_3O_2 at a A99/Cusil ABA interface that was held at 845°C for 300 min.

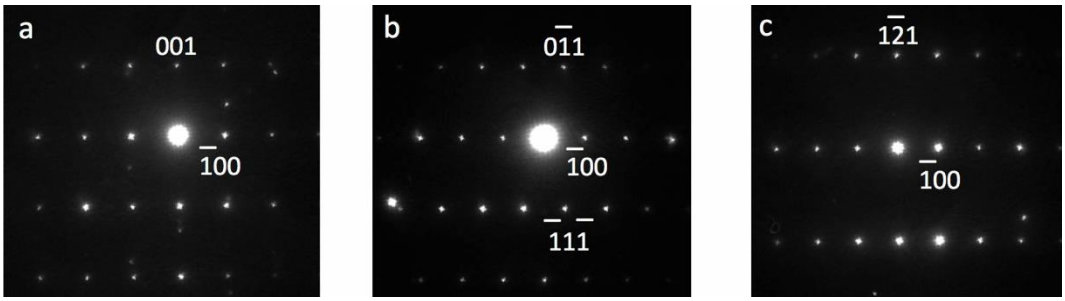

Figure 9. Electron diffraction patterns from Ti_3O_2 with the zone axes a) [010], b) [011] and c) [012].

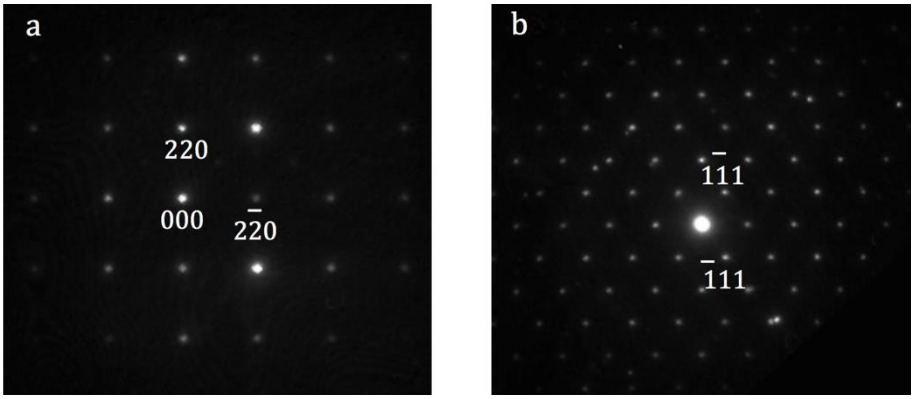

Figure 10. Electron diffraction patterns from Ti_3Cu_3O with the zone axes a) [001] and b) [110].

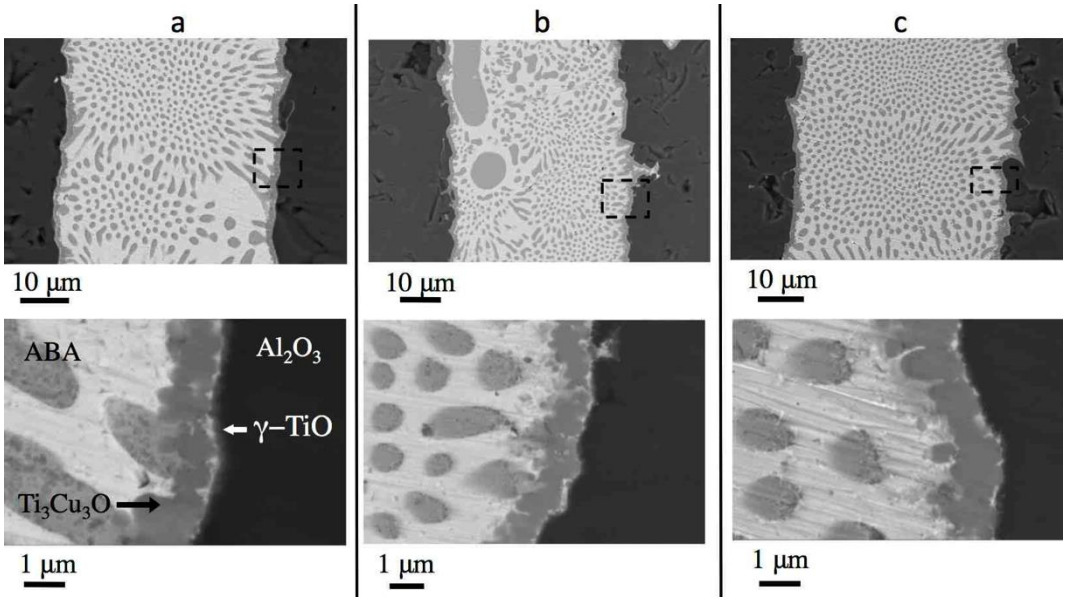

Figure 11. Reaction layers at the Cusil ABA/Al_2O_3 interface after heating to 845°C and holding for 15 min using ceramics a) A99, b) A95 and c) B95.

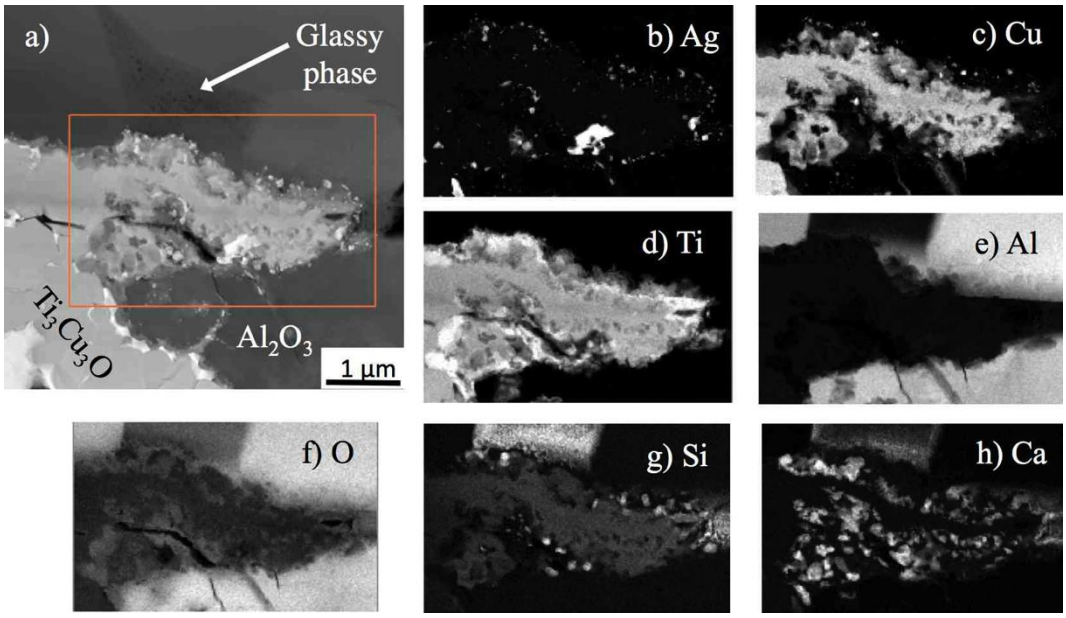

Figure 12. a) HAADF image of a region of Cusil ABA/B95 interface where the ABA has wet and reacted with a calcium silicate glassy phase; the interface was held at 845°C for 15 min. The distributions of Ag, Cu, Ti, Al, O, Si and Ca are given in their X-ray maps (b-h).

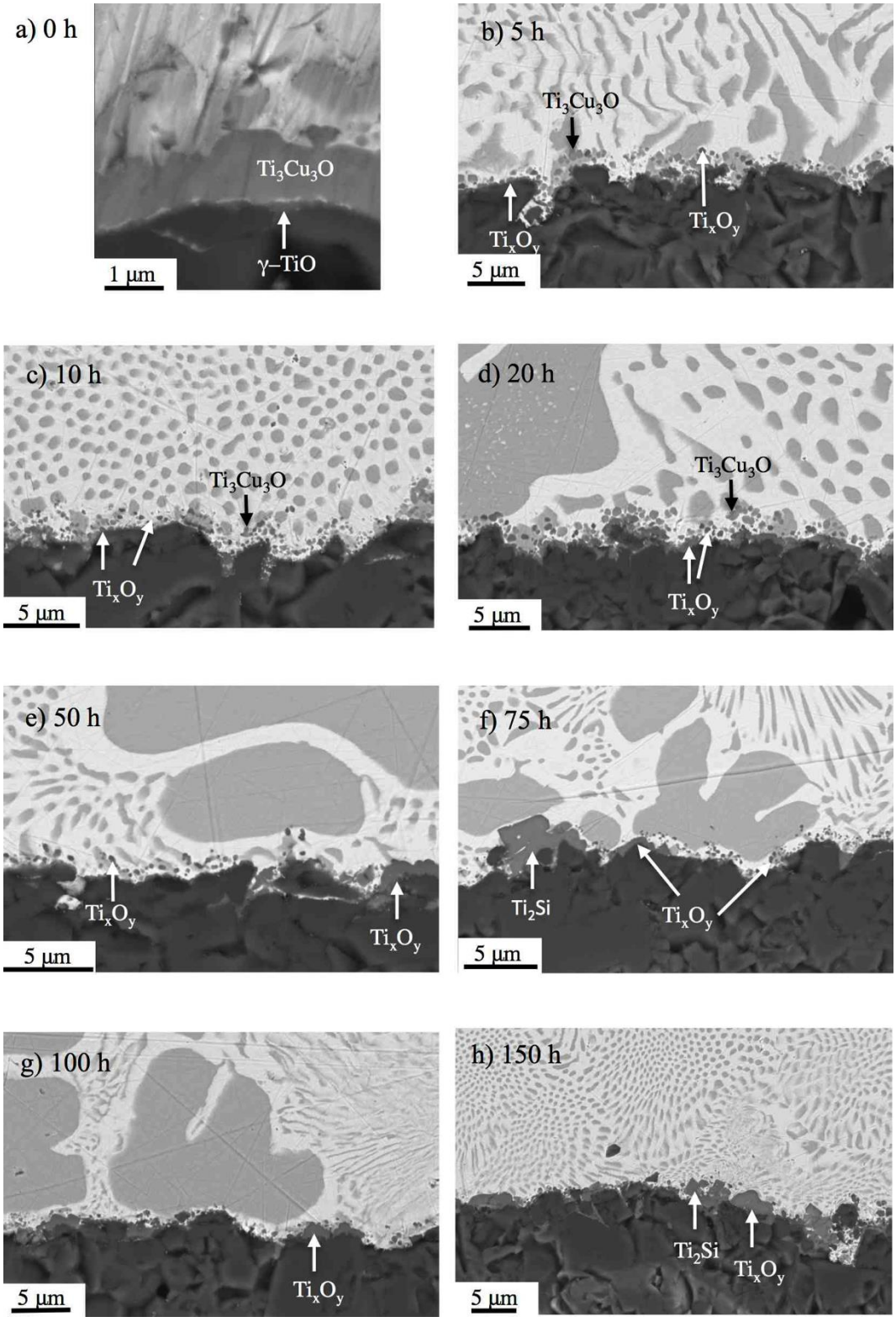

Figure 13. a) BSEI of a Cusil ABA/B95 interface prepared at 815°C for 2 min and cross-sections of this joint after heat to 815°C in Ar gas and holding for b) 5 h, c) 10 h, d) 20 h, e) 50 h, f) 75 h, g) 100 h and h) 150 h.

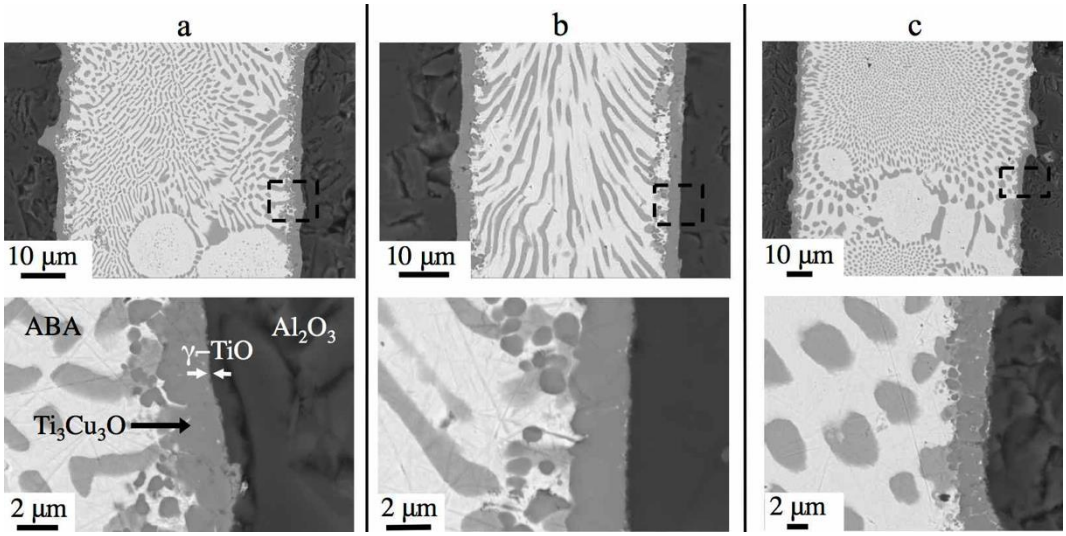

Figure 14. Reaction layers at the Ticusil/B95 interface after holding at 900°C for a) 2 min, b) 15 min and c) 30 min.

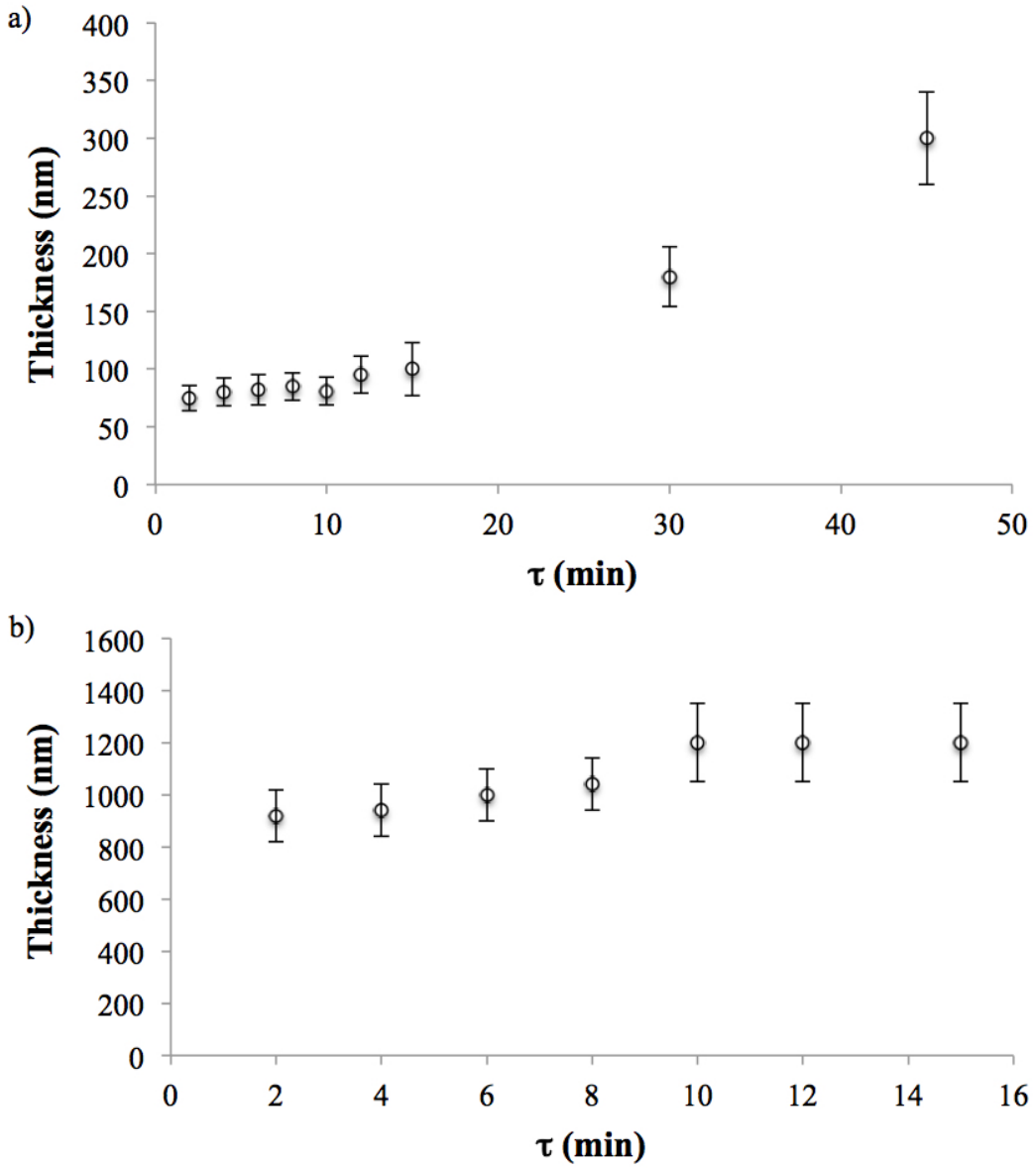

Figure 15. Thicknesses of the a) γ−TiO and b) Ti_3Cu_3O layers at a T_p of 815°C as a function of τ.